PIV analysis of skin friction and coherent structures in turbulent drag reduction regimes

Scarano, F.; Ujjaini Kempaiah, K.; Kotsonis, M.

Publication date
2022

Document Version
Submitted manuscript

Published in
20th International Symposium on the Application of Laser and Imaging Techniques to Fluid Mechanics

PIV analysis of skin friction and coherent structures in turbulent drag reduction regimes

Fulvio Scarano[1,*], Kushal U. Kempaiah [1], Marios Kotsonis[1]
1: Dept. of Aerospace Engineering, TU Delft, The Netherlands
* Correspondent author: f.scarano@tudelft.nl

Keywords: drag reduction, skin friction, oscillating wall, plasma actuator, PIV

ABSTRACT

In the present work, planar and tomographic PIV are used to investigate how the organisation of wall turbulence is altered when actuators are operated with the objective of reducing the skin friction drag. When the wall is mechanically oscillated in the spanwise direction, high-resolution planar PIV enable the direct measurement of wall shear and a 15% reduction of skin friction is observed. The use of tomographic PIV enables access to the three-dimensional organisation of low- and high-speed streaks, along with ejection events and associated hairpin vortices. These observations help forming a conceptual model of the salient drag reduction mechanism, whereby hairpin auto-generation is inhibited through a tilting action at the tail of low-speed streaks.

The second part of the study documents an effort to surrogate the mechanical oscillation by means of a densely distributed array of AC-DBD plasma actuators. The latter are first characterised in quiescent flow, where the induced velocity distribution is obtained and compared to the solution of the classical second Stokes problem that models the mechanical oscillation. The induced peak of spanwise velocity is found to surpass the velocity of the oscillating wall. However, the wall jet height develops further away from the wall. More importantly, the spatially inhomogeneous distribution of the unsteady body force produces an unwanted lattice of starting streamwise vortices. The latter are deemed to be detrimental for the purpose of drag reduction, compared to the orderly and homogeneous sideways motion induced by mechanical wall motion. The application of the AC-DBD actuator currently leads to a pronounced momentum deficit in the logarithmic region and increases skin friction. Finally, further research directions are anticipated, that potentially circumvent the formation of streamwise vortices by means of AC-DBD actuators operating in steady regime.

1. Introduction

Skin-friction is a relevant component of the overall aerodynamic resistance in several engineering systems, notably in aviation, maritime and ground transport. Much research has been devoted to understand ways to mitigate skin friction drag (Choi et al. 1994). A first approach may consist in

delaying the phenomenon of laminar to turbulent transition (Joslin, 1998). When the turbulent regime is fully established, control of turbulent skin friction (or turbulent drag reduction, TDR) has been rigorously investigated, using both passive and active techniques (Gad-el-Hak 1996). Among the many approaches, early works have shown that skewing turbulent motions at the wall (Sendstad et al. 1992) weakens their quasi-streamwise organisation, in turn affecting turbulence production. Since then, much work has been committed to characterise and understand TDR by means of spanwise wall oscillations and surrogates of it.

Numerical studies conducted by Quadrio and Sibilla (2000), alongside experimental works (Choi et al. 2002, Di Cicca et al. 2002) have reported a reduction up to 45% in skin friction, identifying criteria for optimum performance, based on normalised spanwise wall oscillation amplitude $A_{osc}^{+} \geq 100$ and time period $T_{osc}^{+} \approx 100$ (Quadrio and Ricco 2004).

Thereby, the proposed physical mechanism was based on wall motion affecting the orientation of the streamwise vortices (Di Cicca et al. 2002, Touber and Leschziner 2012), in turn disrupting wall-normal turbulent transport. Discrepancies arise when comparing the levels of TDR from different investigations: numerical studies have been typically conducted at relatively low Reynolds number and in a channel flow configuration (Quadrio and Ricco 2004, Touber and Leschziner 2012), whereas experiments were performed over flat-plate turbulent boundary layer (TBL) and at relatively higher values of the Reynolds number (Choi et al 1998, Choi 2002, Di Cicca et al. 2002). The latter have widely employed Hot Wire Anemometry (HWA), yielding detailed velocity profiles and pointwise turbulence spectra. Single-probe measurements, however, lack information on Reynolds stresses and instantaneous vorticity, which prevents visualising the three-dimensional layout of coherent structures. Furthermore, HWA friction measurements are challenged by the oscillating wall.

A recent study conducted with planar and tomographic PIV over the spanwise oscillating wall (Kempaiah et al. 2020) has delivered direct wall shear measurements alongside the visualisation of coherent structures arrangement by 3D vorticity and Q-criterion (Hunt et al. 1988) visualisations. In the above work hairpin vortices, organised by packets (Christensen and Adrian, 2001) of 3 to 5 are most frequently observed as "horse-riding" low-speed flow regions close to the wall. An illustration of this mechanism is given in Fig. 1, following Kempaiah et al. (2020). A main conclusion of the work was that the hairpin packets appear less frequently and with a smaller number of vortices in some wall oscillating regimes.

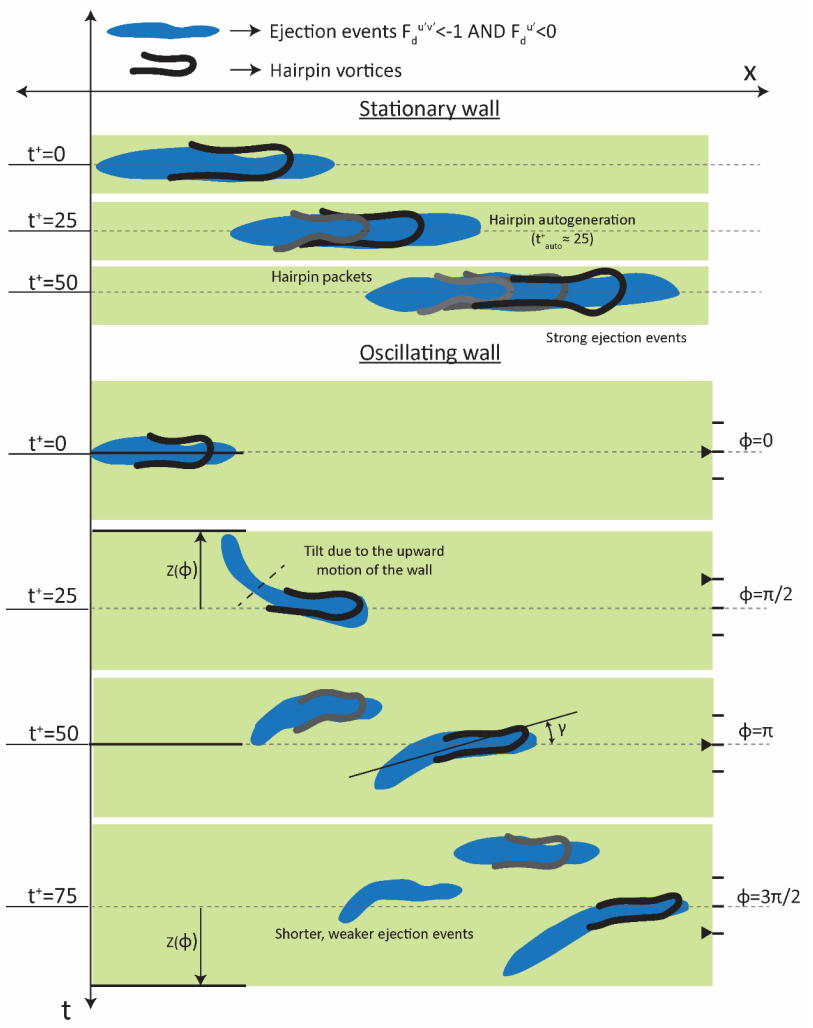

Fig. 1 Schematic illustration of flow ejection events and hairpin vortices arrangements in a turbulent boundary layer with stationary (top) and laterally oscillating wall (bottom). In the latter case, the distortion of the "tail" is shown along the four phases of oscillation. (adapted from Kempaiah et al. 2020)

The use of plasma forcing for skin-friction reduction by surrogating the oscillating wall was analysed by Wilkinson et al (2003), where an oscillatory discharge of weakly ionized surface plasma was used. The results indicated that the strength of the plasma was not sufficient to achieve drag reduction. Jukes et al. (2004, 2006) employed AC-DBD plasma actuators and reported levels of drag reduction up 45% in a turbulent boundary layer with external velocity of 1.8 m/s by generating a bi-directional laminar jet with maximum wall velocity of 2.1 m/s. Furthermore Thomas et al. (2019) employed pulsed DC-DBD actuators and achieved a drag reduction up to 70% at free stream velocity of 17 m/s, leading to a net power saving of 300%. More recent experiments conducted by Hehner et al. (2020) have been successful in replicating the flow induced by the oscillating wall, by employing the beat frequency concept. However, the drag reduction has not been quantified yet for this actuator concept.

The present study first discusses the instantaneous organisation of such coherent structures in the boundary layer in TDR regimes. Vortex visualisations in 2D and 3D are employed to identify the physical mechanism responsible for the skin friction reduction. In the second part of the work, novel experiments are presented, where the mechanical wall oscillation is surrogated by means of a densely distributed array of AC-DBD plasma actuators (Kotsonis, 2015), following the approach of Hehner et al. (2019). In this case, attention is placed on the topology of the flow forced by the actuator and the effects of secondary flows are scrutinised.

2. Turbulent flow over the oscillating plate

The characteristic properties of the turbulent flow developing over an oscillating plate can be divided into two categories: first the properties of the turbulent boundary layer as the external velocity U_∞, the layer thickness δ_{99}, the wall friction τ_w and the viscous length scale y^+. The latter are obtained by means of planar PIV measurements. The properties of the actuator are the oscillation frequency f_{osc}, amplitude A_{osc}, and maximum velocity W_{max}. When scaled to the boundary layer viscous length scale and velocity scale, the latter are denoted as f^+ (or its inverse T^+), A^+ and W^+.

2.1 Experimental apparatus and PIV measurements

Experiments were conducted in the open-return low-speed facility *W*-tunnel at the faculty of aerospace engineering of TU Delft. The boundary layer is tripped close to the leading edge and develops along a 1.5 m long flat plate. The oscillating section is placed 1.3 m past the tripping device. Two-components (X-Y) planar PIV and three-dimensional tomographic PIV measurements are performed for the study of the wall friction and of the topology of coherent flow structures. Details of the experimental setup, data acquisition and PIV processing parameters are given in Kempaiah et al. (2020). The turbulent boundary layer properties obtained from planar-PIV data are summarised below, followed by the illustration of the experimental arrangement.

Table 1: Turbulent boundary layer properties

Re_θ	Re_τ	U_∞ [m/s]	δ_{99} [mm]	δ^* [mm]	θ [mm]	u_τ [m/s]	y^+ [mm]	H
980	570	3.0	59.0	6.7	4.9	0.145	0.10	1.36

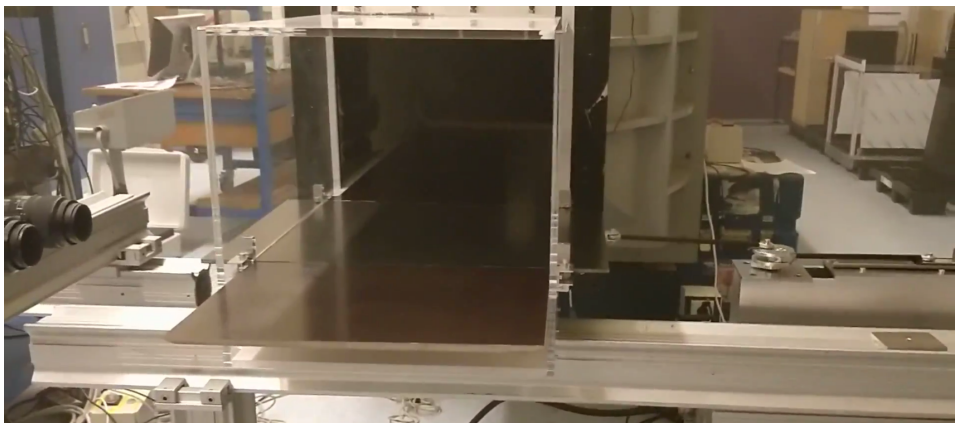

Fig. 2 W-tunnel test section with flat plate and oscillating wall segment (in black). The mechanical actuator is visible on the right side, whereas PIV cameras are placed on the left side.

The measurement volume for tomographic-PIV is placed 25 cm downstream of the leading edge of the oscillating wall, with the dimensions of $7 \times 6 \times 0.6$ cm^3 along streamwise, spanwise and wall-normal directions respectively. The average imaging magnification is $M = 0.2$ with a digital resolution of 32 pixels/mm. The instantaneous particle distribution was reconstructed with the CSMART tomographic algorithm with five iterations. The cross-correlation analysis returns $293 \times 246 \times 24$ velocity vectors using an interrogation volume size of $32 \times 32 \times 32$ voxels giving a vector spacing of 0.25 mm (2.5 wall units) with 75% overlap. A total of 400 recordings is taken for the purpose of phase-averaged and ensemble statistical analysis.

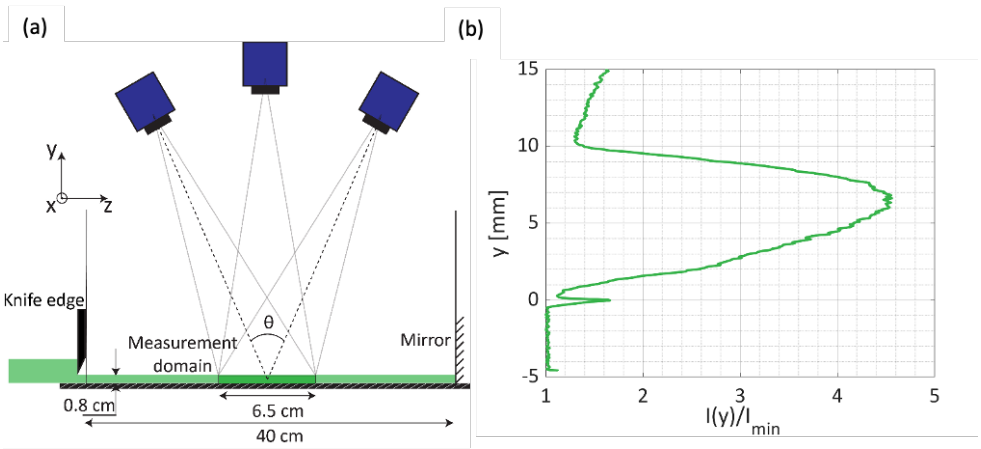

Fig. 3 Illustration of the tomographic system arrangement (a); Reconstructed particle light intensity I(y), in the wall normal direction (normalized to the minimum value (I_{min}) (b).

2.2 Altered organization of coherent structures

The tomographic measurement volume encompasses the buffer layer ($y+$ = 20–70) enabling the visualization of the near-wall streamwise velocity distribution ($y+$ = 20). Fig. 4 shows the streaky pattern given by a series of elongated low-speed regions with spanwise separation of ~100 $y+$, and a varying length (600 - 850 $y+$), which agrees with literature data (Kline et al. 1967; Kähler 2004). Furthermore, flow ejections correlate consistently with the low-speed flow regions as also reported in several previous works. At higher distance from the wall the streamwise coherence decays and these regions appear wider and often interrupted.

The streamwise velocity contours for the oscillating wall indicate that oscillations lead to a significant weakening of the streamwise coherence. In this case, also the ejection regions are more sparsely observed and are less consistent with the low-speed streaks. A tilted tail of the low-speed regions, as a result of the oscillatory motion, can be observed when inspecting the flow field corresponding to a given phase of the oscillation.

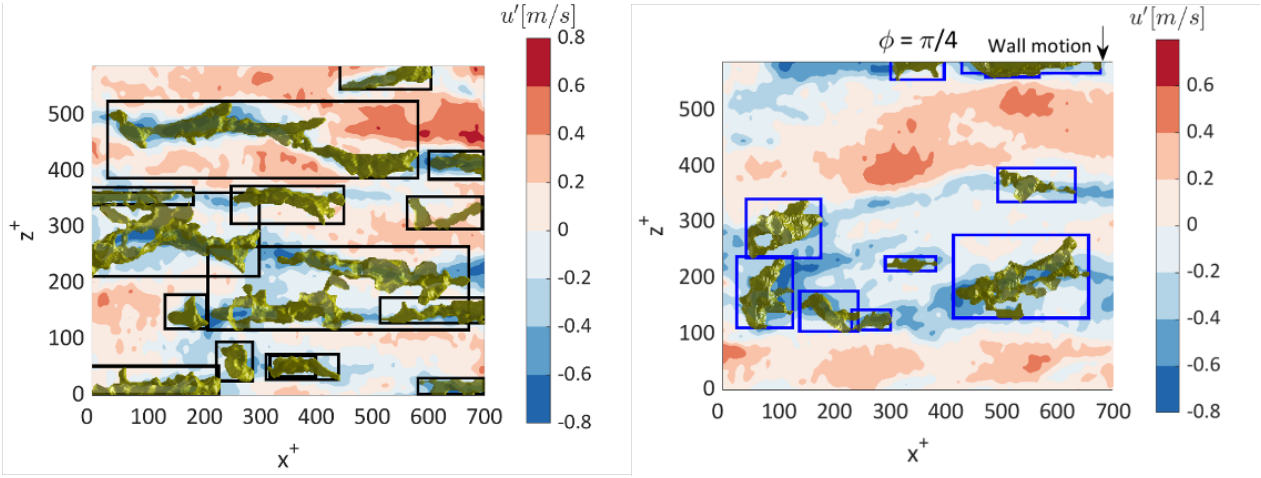

Fig. 4 Visualisation of instantaneous streamwise velocity and iso-surfaces of ejection events ($u'v' < 0$) for the stationary (left) and oscillating wall (right). Flow direction is left to right.

Fig. 5 illustrates an instantaneous sample of the vortical structures as they often appear in the undisturbed boundary layer and while the wall is oscillated. Elongated regions of vertical velocity are prominent and coherent in the undisturbed turbulent regime. Some remnant of such structures is visible during wall oscillation. However, their coherence and intensity are much reduced. Hairpin vortices and connected hairpin legs densely populate the low-speed regions, participating the action of the vertical ejections. When the wall is oscillated, such structures appear less frequently and more isolated, with significantly less focused effect on the ejections' mechanism.

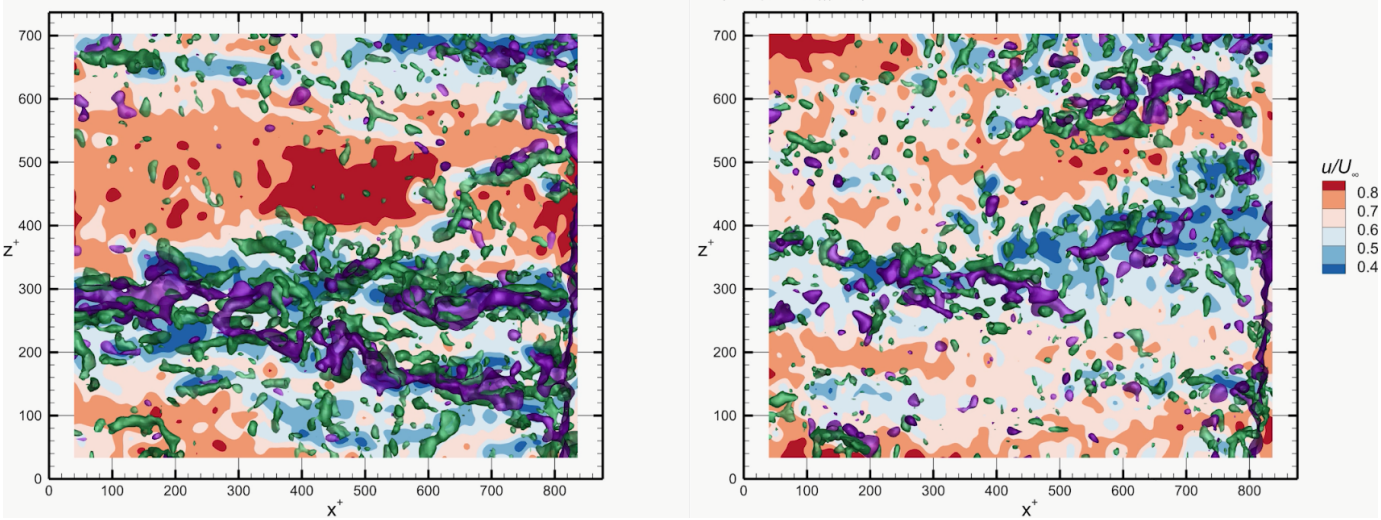

Fig. 5 Visualisation of instantaneous streamwise velocity, iso-surfaces of vertical velocity (purple) and of vortical structures (green) for the stationary (left) and oscillating wall (right). Flow direction is left to right.

Evidence of reduced skin friction drag is obtained by direct inspection of the wall shear. Tomographic PIV does not allow the analysis at the needed spatial resolution to describe the viscous layer and in particular the linear region. The latter is accessed with high-resolution (12 vectors/mm) two-components PIV. Fig. 6 illustrates the measurement range obtained with planar and tomographic PIV in the investigation of Kempaiah et al. (2020) and compared with a numerical simulation presented by Schlatter and Örlü (2010).

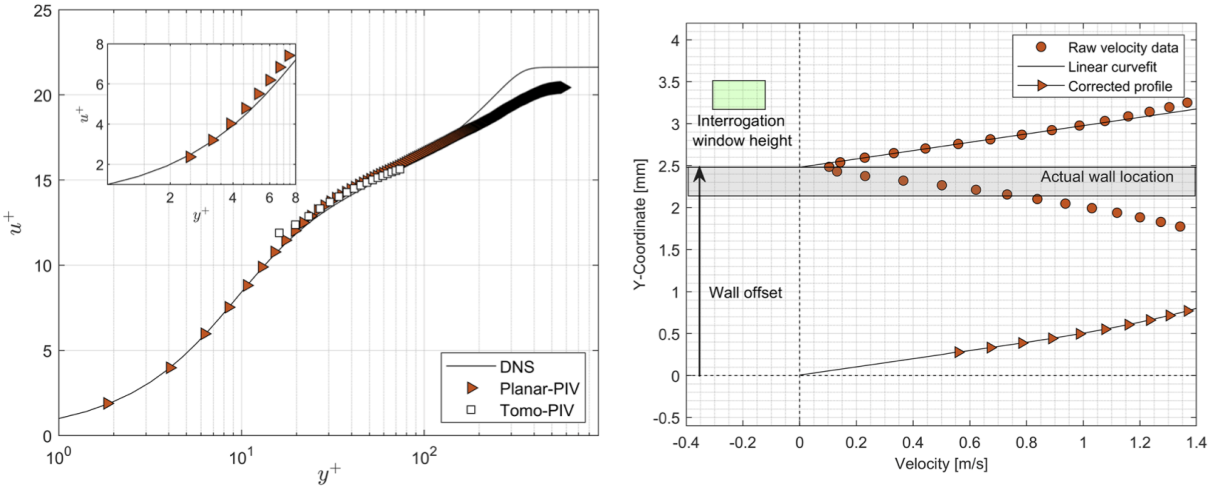

Fig. 6 Wall-normal measurement range obtained by planar and Tomo PIV (left). Detail of near wall velocity analysis for wall shear measurement. (Wall position identified by reflected particles image). Kempaiah et al. (2020).

In the present experiments, the largest drag reduction (15 %) has been found with wall oscillations at amplitude of 1 cm ($A^+ = 100$) and an oscillation period of 67 ms ($T^+ = 95$). A further, high-resolution visualisation of the instantaneous spanwise vorticity (Fig. 7) reveals the large differences in the flow structures discussed above when the wall is oscillating under the above conditions. The number of hairpins observed to form elongated and connected packets is significantly reduced, in agreement with the scenario depicted in Fig. 1 and Fig. 5.

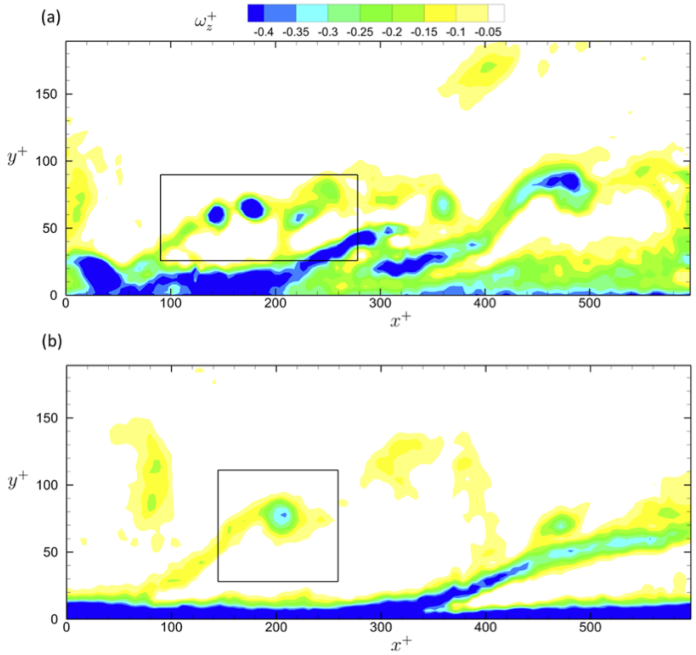

Fig. 7 Instantaneous spanwise vorticity distribution revealing multiple hairpins packet for the stationary wall (a) and more isolated structures for the oscillating wall (b). (Kempaiah et al. 2020).

3. Surrogate of mechanical oscillation by plasma actuators

Although proven effective, mechanical oscillation of the wall to reduce skin friction drag offers little to no perspective for direct engineering applications that aim at improving the energy efficiency of transport systems. An alternative route towards applications of this drag reduction mechanism is illustrated here, where the mechanical actuator is replaced by an electrical system that surrogates the behaviour of the flow near the wall. A plasma actuator based on alternating current dielectric barrier discharge (AC-DBD, Corke et al. 2010) is designed to surrogate the wall motion by a thin and homogenous wall jet. The following sections describe the actuator, its operations and the flow field produced by it, at conditions similar to those of the oscillating wall.

3.1 Actuator layout and operations

AC-DBD actuators with varying exposed (L_1), covered (L_2) electrode lengths and spacing (L_3) were manufactured. The electrodes were obtained using a novel inkjet printing of silver ink on specially treated polyethylene terephthalate (PET) foils (Peng and Kotsonis 2021), sandwiched between a sheet of Poly(methyl methacrylate) (PMMA) dielectric of varying thickness (t). The above parameters were varied such to achieve a close surrogate to the oscillating wall conditions reported in Kempaiah et al (2020). The variables that determined the actuator configuration were geometrical (L_1, L_2, L_3 and t) and electrical (voltage (V), frequency (f) and wave form).

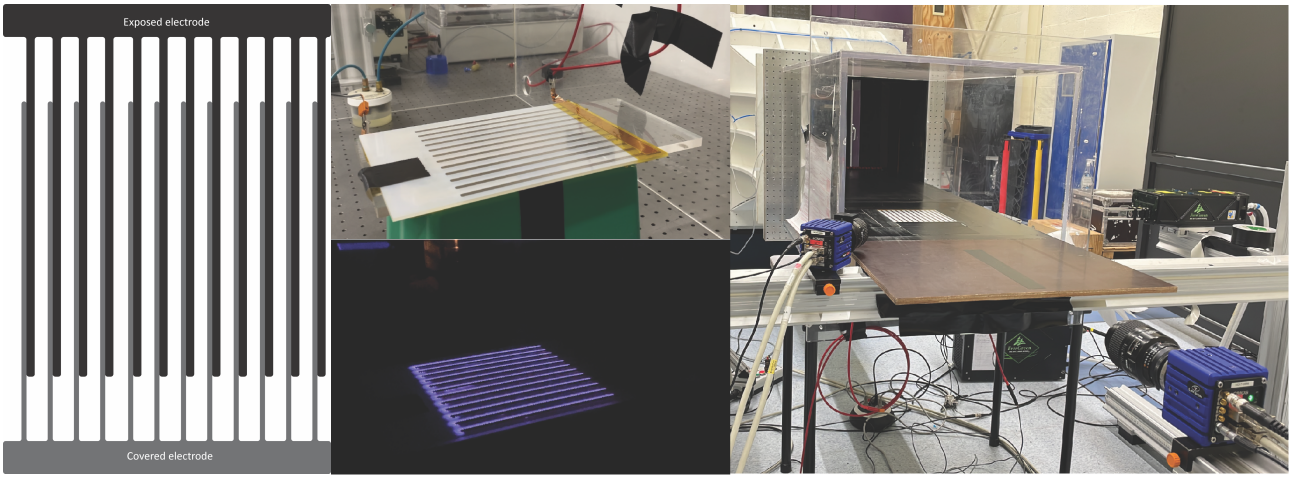

Fig. 8 Layout of plasma actuator (left) and its operation in the quiescent flow experiment (middle-top) while glowing (middle-bottom). Plasma actuator installation in the boundary layer facility (right).

Based on a systematic planar-PIV investigation, the suitable exposed and covered electrode lengths were finalised to be $L_1 = 5$ mm and $L_2 = 3$mm with spacing of $L_3 = 6$ mm, with a dielectric thickness of 3 mm. An input signal corresponding to AC voltage of 30 kV, peak-peak frequency of 28kHz and duty cycle of 50% was chosen. The experimental investigations to achieve the required actuator configuration were performed in two steps: first under quiescent flow conditions (
Fig. 8-left); secondly, the actuator was installed in the TBL flow (
Fig. 8-right).

3.2 Similarity of forcing

Here, attention is placed on the topology of the flow forced by the actuator and the effects of secondary flows are scrutinised. When the flow velocity is averaged in the spanwise direction the

velocity profile can be compared with that of the oscillating wall obtained through the Stokes problem at T^+={0, ¼, ½, ¾}. The velocity produced by the plasma actuator peaks at 2.5 m/s, which is larger than that of the oscillating wall at T^+=95 and A^+=100, which peaks at 1 m/s at the wall. However, two main differences can be observed: first, the velocity at the wall remains null; secondly, the sideways velocity features a wall jet with peak between 1 and 3 mm off the wall, depending on the considered actuation phase (Fig. 9).

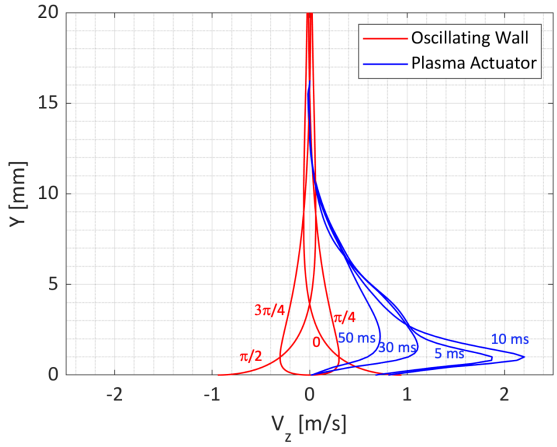

Fig. 9 Modelled velocity profile during mechanical wall oscillation (red) and velocity measured during plasma actuation (blue).

The instantaneous spanwise velocity field is shown in Fig. 10. Owing to the inhomogeneous and unsteady nature of the actuation, the formation of a starting vortex cannot be avoided (Fig. 10). Such motions are undesired as they initiate vertical motions and momentum mixing across the boundary layer.

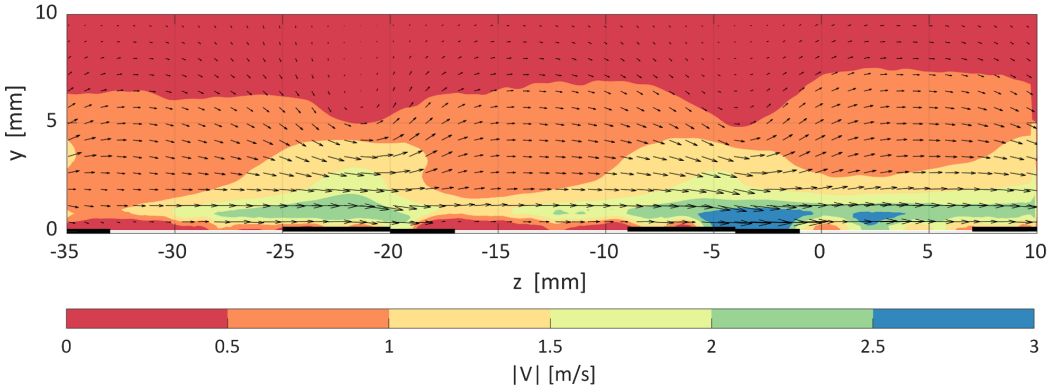

Fig. 10 Instantaneous velocity field induced (spanwise) by the plasma actuator after 10 ms.

The same actuator was immersed in a TBL to assess its skin friction reduction capabilities. The velocity profile of the TBL subjected to the plasma forcing resulted in a large deficit in momentum

in the log-region (Fig. 11-left). A detailed analysis near the wall reveals that the wall shear force is not decreased, instead increases visibly (Fig. 11-right). The latter effect is ascribed to the formation of additional flow structures (streamwise vortices) resulting from the unsteady and inhomogeneous actuation. The present results are in contrast with the works of Jukes et al (2006) were drag reductions up to 45% were reported.

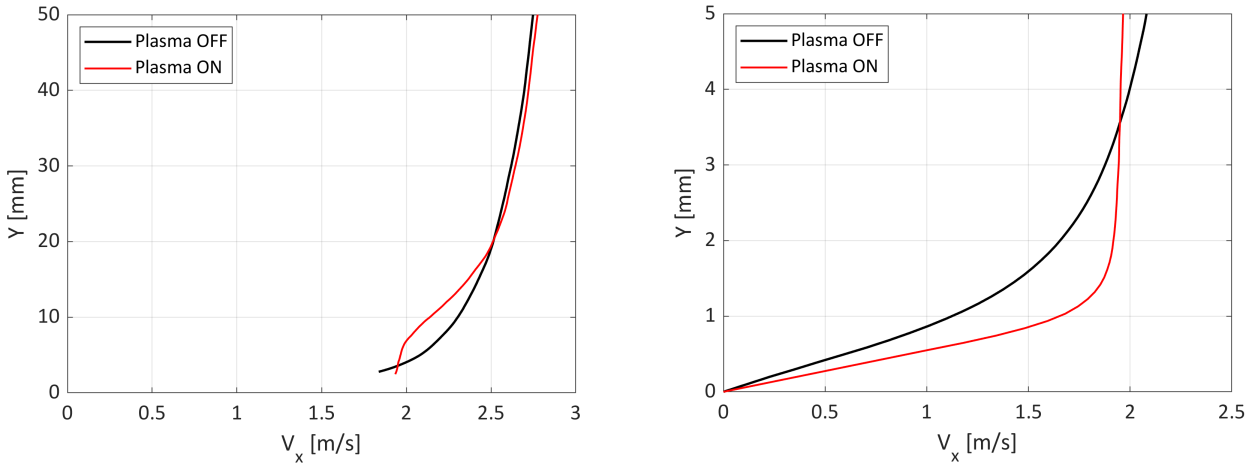

Fig. 11 Velocity profile in the boundary layer with and without plasma actuation. A pronounced deficit region is produced in the log-layer (left) with inversion close to the wall (right) leading to increased skin friction.

Although the conditions are not exactly replicated, the arrangement of plasma actuators and the operating range are somewhat similar. In the work of Jukes et al (2006), a working principle for skin friction reduction is proposed where the streamwise vortices play a role. However, the structure of instantaneous three-dimensional velocity and vorticity remains to be ascertained and understood, which remains open for further investigations.

Therefore, the role of unsteady streamwise vortices on skin friction control requires further understanding, possibly to guide towards approaches that avoid their occurrence. The latter cannot be overcome due to the physical principle of plasma body forces being formed by discrete electrodes. Some potential is seen in adopting a steady actuation principle, that yet mimics the effects observed with the mechanical wall oscillation. Also in this case, further studies are being devoted in the realisation of such actuation principle as also indicated in Quadrio et al (2009), who report an optimal spatial amplitude (analogous to the time period in temporal oscillation) λ^+ close to 1000 wall units. The latter corresponds to 10 cm for the TBL at Re = 1500. Current research is realising such actuators, where the streamwise extent is limited by the size of the printable area for the array i.e. A4 (21.0 × 29.7 cm). A sample of the actuator and its operation in quiescent flow are illustrated in Fig. 12.

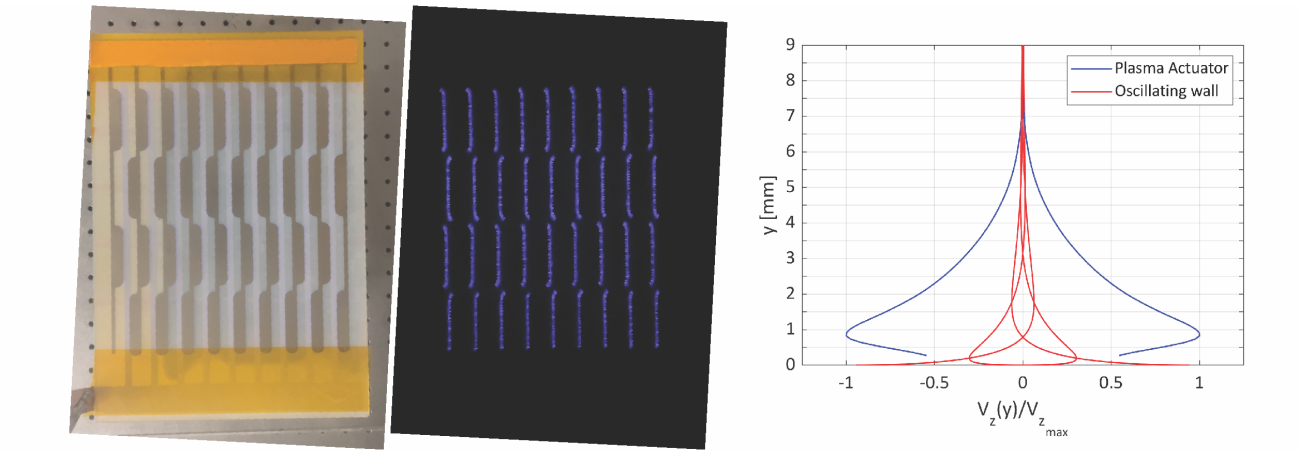

Fig. 12 Plasma actuator layout (left) and active regions during operation (middle). Comparison between Stokes layer and measured velocity during the actuator steady operation (right).

4. Conclusions

This work documents the research advancements towards the realisation of active flow control for turbulent drag reduction. Different devices to obtain a drag reduction are inspected that are based on the principle of imposed spanwise oscillations. The physical principle is introduced as a distortion of the low-speed streaks where ejection events are dominated by the collective action of hairpin vortices organised along packets. Such distortion is ascribed to the separation at the tail of the packet of hairpins still to be developed, which interrupts or at least inhibits the auto-generation mechanism. The use of high-resolution PIV enables the direct measurement of the skin friction by identifying the linear velocity profile in the viscous sub-layer. Furthermore, tomographic PIV illustrates that the number of hairpins connected in a packet is visibly reduced under the optimal regime of oscillation.

The use of plasma actuators to produce a similar effect is further documented in this work. A dense array of AC-DBD plasma actuators to produce a rather homogeneous sideways forcing of the near wall fluid is investigated, first in quiescent conditions and after in the TBL. The unsteady actuation in combination with the discrete nature of the body force distribution produces streamwise vortices that modulate the flow spanwise. The latter results in increased skin friction and a momentum deficit in the logarithmic layer. These result somehow contrast with some literature work that reports large reduction of skin friction drag with a similar arrangement of plasma actuators, which justifies further efforts with 3D flow diagnostics to experimentally characterise these flow regimes.

References

Adrian, R. J. (2007). Hairpin vortex organization in wall turbulence. *Physics of Fluids*, 19, 041301

Choi H., Moin P., & Kim J. (1994). Active turbulence control for drag reduction in wall-bounded flows. *Journal of Fluid Mechanics*, 262, 75 – 110

Choi, K.-S., DeBisschop, J.-R., & Clayton, B. R. (1998). Turbulent boundary-layer control by means of spanwise-wall oscillation. *AIAA Journal*, 36, 1157–1163

Choi, K.-S., (2002). Near-wall structure of turbulent boundary layer with spanwise-wall oscillation. *Physics of Fluids*, 14

Christensen, K. T., & Adrian, R. J. (2001). Statistical evidence of hairpin vortex packets in wall turbulence. *Journal of Fluid Mechanics*, 431, 433-443

Corke, T. C., Enloe, C. L., & Wilkinson, S. P. (2010). Dielectric barrier discharge plasma actuators for flow control. *Annual Review of Fluid Mechanics*, 42, 505-529

Di Cicca, G. M., Iuso, G., Spazzini, P. G., & Onorato, M. (2002). Particle image velocimetry investigation of a turbulent boundary layer manipulated by spanwise wall oscillations. *Journal of Fluid Mechanics*, 467, 41–56

Elsinga, G. E., Scarano, F., Wieneke, B., & van Oudheusden, B. W. (2006). Tomographic particle image velocimetry. *Experiments in Fluids*, 41, 933–947

Gad-el-Hak, M. (1996). Modern developments in flow control. *Applied Mechanics Reviews*, 49, 365–379

Hehner, M. T., Gatti D., & Kriegseis J. (2019). Stokes-layer formation under absence of moving parts—A novel oscillatory plasma actuator design for turbulent drag reduction. *Physics of Fluids*, 31, 051701

Hehner, M.T., Gatti, D., Mattern, P., Kotsonis, M., & Kriegseis, J. (2020). Virtual wall oscillations forced by a DBD plasma actuator operating under beat frequency - a concept for turbulent drag reduction. *AIAA Aviation 2020 Forum*, 2956

Hunt, J. C. R., Wray, A. A., & Moin, P. (1988). Eddies streams and convergence zones in turbulent flows. *Center for Turbulence Research Summer Program*

Jodai, Y., & Elsinga, G. E. (2016). Experimental observation of hairpin auto-generation events in a turbulent boundary layer. *Journal of Fluid Mechanics*, 795, 611–633

Joslin, R. D. (1998). Aircraft laminar flow control. *Annual Review of Fluid Mechanics*, 30, 1-291

Jukes, T., Choi, K.-S., Johnson, G., & Scott, S. (2004). Turbulent boundary-layer control for drag reduction using surface plasma. *2nd AIAA flow control conference*, 2216

Jukes, T., Choi, K.S., Johnson, G., & Scott, S. (2006). Turbulent drag reduction by surface plasma through spanwise flow oscillation. *3rd AIAA Flow Control Conference*, 3693

Kähler, C. J., (2004). The significance of coherent flow structures for the turbulent mixing in wall-bounded flows. *Ph.D. dissertation* (DLR, Dt. Zentrum für Luft-und Raumfahrt)

Kempaiah, K. U., Scarano, F., Elsinga, G. E., Van Oudheusden, B. W., & Bermel, L. (2020). Three-dimensional particle image velocimetry based evaluation of turbulent skin-friction reduction by spanwise wall oscillation. *Physics of Fluids*, 32, 085111

Kline, S. J., Reynolds, W. C., Schraub, F. A., & Runstadler, P. W. (1976). The structure of turbulent boundary layers. *Journal of Fluid Mechanics*, 30, 741–773

Kotsonis, M. (2015) Diagnostics for characterisation of plasma actuators. *Measurement Science and Technology*, 26, 092001

Peng, K., & Kotsonis, M. (2021). Cross-flow instabilities under plasma actuation: Design, commissioning and preliminary results of a new experimental facility. *AIAA Scitech 2021 Forum*, 1194

Quadrio, M., & Sibilla, S. (2000). Numerical simulation of turbulent flow in a pipe oscillating around its axis. *Journal of Fluid Mechanics*, 424, 217–241

Quadrio, M., & Ricco, P. (2004). Critical assessment of turbulent drag reduction through spanwise wall oscillations. *Journal of Fluid Mechanics*, 521, 251–271

Quadrio, M., Ricco, P., & Viotti, C. (2009). Streamwise-traveling waves of spanwise wall velocity for turbulent drag reduction. *Journal of Fluid Mechanics*, 627, 161-178

Schlatter, P., & Örlü, R. (2010). Assessment of direct numerical simulation data of turbulent boundary layers. *Journal of Fluid Mechanics*, 659, 116–126

Sendstad, O. (1992). The near wall mechanics of three-dimensional turbulent boundary layers. *Stanford University*

Thomas, F. O., Corke, T. C., Duong, A., Midya, S., & Yates, K. (2019). Turbulent drag reduction using pulsed-DC plasma actuation. *Journal of Physics D: Applied Physics*, 52, 434001

Touber, E., & Leschziner, M. A. (2012). Near-wall streak modification by spanwise oscillatory wall motion and drag-reduction mechanisms. *Journal of Fluid Mechanics*, 693, 150–200

Wilkinson, S.P. (2003). Investigation of an oscillating surface plasma for turbulent drag reduction. *41st Aerospace Sciences Meeting and Exhibit*, AIAA Paper 2003-1023